FTY720 attenuates APAP-induced liver injury via the JAK2/STAT3 signaling pathway

XIANGMIN HE[1], KAI KANG[1], DAN PAN[2], YUE SUN[1] and BING CHANG[1]

Departments of [1]Gastroenterology and [2]Geriatrics, The First Affiliated Hospital, China Medical University, Shenyang, Liaoning 110000, P.R. China

Received August 24, 2021; Accepted January 20, 2022

DOI: 10.3892/ijmm.2022.5123

Abstract. As the current clinical treatment of acetaminophen (APAP)-induced liver injury (AILI) has its limitations, new and effective treatment methods are required. Fingolimod (FTY720) is an immunosuppressive drug developed in recent years that has been shown to have a protective effect against ischemia/reperfusion liver injury. However, the role of FTY720 in AILI remains unclear. The aim of the present study was to determine whether FTY720 has a protective effect on AILI. AILI was induced using intraperitoneal injection of 300 mg/kg APAP in male C57BL/6J mice. Following APAP challenge, the mice were administered 5 mg/kg FTY720 for 30 min. Protein expression levels were measured using western blot analysis. Cell viability was examined using Cell Counting Kit-8 assays. mRNA levels were measured using reverse transcription-quantitative PCR. Inflammation levels were evaluated using immunohistochemistry. Cell death and reactive oxygen species levels were examined using immunofluorescence. Furthermore, laser scanning intravital microscopy was used to directly observe immune cell recruitment. APAP treatment increased the serum levels of alanine transaminase and aspartate transaminase at the 6- and 12-h time-points, suggesting liver tissue damage. However, FTY720 attenuated the liver injury induced by APAP by reducing the recruitment of immune cells and the release of pro-inflammatory cytokines and chemokines. FTY720 activated JAK2/STAT3 signaling and regulated the expression of BAX, BCL-2 and p65 to inhibit apoptosis and inflammation. In addition, compared with APAP treatment, the viability of primary hepatocytes treated with APAP and FTY720 was increased. Inhibition of JAK2/STAT3 signaling attenuated the protective, antioxidant effects of FTY720. In conclusion, FTY720 reduced liver injury by regulating the JAK2/STAT3 signaling pathway. This compound was capable of inhibiting oxidative stress to reduce hepatocyte death and the infiltration of neutrophils in the liver.

Correspondence to: Dr Xiangmin He, Department of Gastroenterology, The First Affiliated Hospital, China Medical University, 155 Nanjing North Street, Heping, Shenyang, Liaoning 110000, P.R. China
E-mail: xiaohe0824@sina.com

Key words: fingolimod, acetaminophen, acetaminophen-induced liver injury, acute liver injury

Introduction

Acetaminophen (APAP) is a widely used analgesic and antipyretic drug (1). Although APAP is generally safe and effective, excessive APAP use can cause severe liver injury that eventually develops into liver failure (2). The APAP-induced liver injury (AILI) animal model displays characteristics similar to those observed in patients and has been widely used to study the mechanisms underlying this condition in order to identify potential therapeutic intervention strategies (3,4). The main pathogenic mechanism of AILI is that excessive APAP produces toxic metabolites of *N*-acetyl-*p*-benzoquinone imine (NAPQI) through cytochrome P450 (CYP) metabolism (mainly CYP2E1). The accumulated NAPQI depletes the intracellular glutathione levels. Any glutathione that is not bound to NAPQI can then bind with mitochondrial membrane proteins, leading to mitochondrial permeability transition. This can directly impair mitochondrial function in hepatocytes, causing lipid peroxidation, oxidative stress and DNA fragmentation, thus resulting in hepatocyte necrosis (5-7). In addition, it has also been shown that, following APAP treatment, a large number of neutrophils infiltrate the site of injury, further aggravating liver damage (8).

Fingolimod (FTY720) is a novel type of immunosuppressive drug derived from the ascomycete *Cordyceps sinensis* (9). Different from conventional immunosuppressive compounds, such as cyclosporine, tacrolimus and sirolimus, FTY720 acts by inducing lymphocyte apoptosis and homing (10). FTY720 is a sphingosine-1-phosphate (S1P) analogue, which can be phosphorylated by sphingosine kinase. Phosphorylated (p)-FTY720 is transported by S1P transporter proteins across the membrane to the outside of the cell and competitively binds to the S1P receptor, thus antagonizing downstream S1P signaling (11).

The JAK2/STAT3 signaling pathway can be activated by various cytokines and participates in numerous important biological processes, such as cell proliferation, differentiation and immune regulation (12-14). Previous studies have found that hepatocyte necrosis was closely related

to the JAK2/STAT3 signaling pathway (15-17). However, it is unclear whether FTY720 exerts its immunosuppressive effect through the JAK2/STAT3 signaling pathway. Therefore, in order to further explore the preventive and therapeutic effect of FTY720 *in vivo*, an AILI animal model was used. The specific mechanism underlying the effect of FTY720 on the liver was evaluated by examining serum liver function markers and pathological changes in hepatocytes (18-20).

Materials and methods

Experimental animals and experimental design. Male C57BL/6 mice (8-9 weeks of age) were purchased from the Animal Experimental Center of China Medical University (Shenyang, China) and housed in a pathogen-free environment (temperature, 23±2˚C; humidity, 55±5%) with a 12-h light/dark cycle and free access to food and water. Mice weighing 18-22 g (a total of 192 mice; 64 mice used for 3 cycles of experiments) were randomly separated into four groups after overnight fasting as follows: i) Control group, mice were administered 200 μl PBS; ii) FTY720 group, mice received 5 mg/kg FTY720 [Cayman Chemical Company; molecular formula, $C_{19}H_{34}NO_5P$ (Fig. 1A); molecular weight, 387.5; purity ≥98%; solubility in chloroform, 0.5 mg/ml; slightly soluble in DMSO)] intraperitoneally (i.p.); iii) APAP group, mice received 300 mg/kg APAP (MilliporeSigma) i.p.; and iv) FTY720 + APAP group, mice were administered FTY720 again after APAP challenge for 30 min. Mice were anesthetized with 200 mg/kg ketamine and 10 mg/kg xylazine i.p., then euthanized 6 h (n=8/group) or 12 h (n=8/group) after APAP injection. Serum was collected and livers were harvested. In addition, AG490 was used to inhibit the JAK2/STAT3 signaling pathway in mice. Mice weighing 18-22 g (a total of 120 mice; 30 mice used for 3 cycles of experiments) were randomly separated into four groups after overnight fasting as follows: Each group received 300 mg/kg APAP i.p; i) Control group, mice were administered 200 μl PBS; ii) FTY720 group, mice received 5 mg/kg FTY720; iii) AG490 group, mice received 50 μM AG490; and iv) FTY720 + AG490 group, mice were administered FTY720 and AG490 again after APAP challenge for 30 min. Mice were anesthetized with 200 mg/kg ketamine and 10 mg/kg xylazine i.p., then euthanized 6 h (n=10/group) or 12 h (n=8/group) after APAP injection. Serum was collected and livers were harvested. The experimental protocols were approved (approval no. CMU2021076) by the Institutional Animal Care and Use Committee and conformed to the Guidelines for the Care and Use of Laboratory Animals of China Medical University (Shenyang, China).

Liver histopathology. The mice were anesthetized with 200 mg/kg ketamine and 10 mg/kg xylazine i.p., then sacrificed by cervical dislocation. For histopathological examination, the liver tissues were fixed in 10% formalin at 25˚C for 24 h, then embedded in paraffin, sectioned at 5-μm thickness and stained with H&E at 25˚C for 10 min. To estimate the extent of necrosis, the specimen was observed under a light microscope, using ImageJ software (version 1.8.0; National Institutes of Health) to calculate the necrotic area.

Immunohistochemistry. Paraffin tissue sections of mouse livers were baked at 60˚C for 1 h. Next, the samples were dewaxed in gradient xylene, and placed in water after dewaxing. Subsequently, 10 parts of distilled water to 1 part of 30% H_2O_2 was added, and then the sections were washed 3 times with distilled water at room temperature for 10 min each time. The sections were then immersed in 0.01 M citric acid buffer, heated to boiling at maximum power in a microwave (98-100˚C), cooled (5-10 min), and repeated twice. The slices were cooled naturally at room temperature and washed 3 times with PBS for 5 min each time. Next, the sections were sealed with 5% BSA at room temperature for 20 min, and excess liquid was removed. The primary antibody (F4/80; 1:500; product no. 70076; Cell Signaling Technology, Inc.) was then added dropwise at 37˚C for 1 h or 4˚C overnight. The sections were then washed 3 times with PBS for 3 min each time. Subsequently, the secondary antibody (HRP-conjugated goat anti-mouse IgG; product no. 91196; 1:5,000; Cell Signaling Technology, Inc.) was added dropwise at 37˚C for 15-30 min. The sections were then washed 3 times with PBS for 3 min each time. The streptavidin-biotin complex (SABC) was then added dropwise at 37˚C for 30 min. Next, the sections were washed 3 times again with PBS for 5 min each time. The color developing agent was then added dropwise in 1 ml distilled water and mixed well. After the DAB chromogenic agent was prepared, it was added onto the sections at room temperature, and the reaction time was observed under a microscope (~5 min). The sections were then rinsed with tap water and then with distilled water. The sections were counterstained with hematoxylin for 2 min and then rinsed with tap water. Finally, the film was sealed by gradient dehydration and neutral resin. The film was observed and images were captured under a light microscope (OLYMPUS IX73; Olympus Corporation).

Plasma assay. Plasma alanine transaminase (ALT; cat. no. C009-2-1), aspartate transaminase (AST; cat. no. C010-2-1) and albumin (ALB; cat. no. A028-2-1; all from Nanjing Jiancheng Bioengineering Institute), and total bilirubin (TBIL) activities (cat. no. Hhzt-4576; Shanghai Huzheng Biology Pharmaceutical Co., Ltd.) were measured according to the manufacturer's protocol.

Myeloperoxidase (MPO) ELISA. The levels of MPO in the liver tissue were determined using an MPO ELISA kit [cat. no. ZC-38698; Shanghai Zhuo Cai Technology Co., Ltd. (ZCIBIO)] according to the manufacturer's protocol. Briefly, liver tissue samples were washed with PBS and homogenized in RIPA (cat. no. 89900; Thermo Scientific, Inc.) buffer using a tissue homogenizer (Ultra-Turrax). The homogenate was then centrifuged at 5,000 x g for 5 min at 4˚C and immediately used for ELISA. The sample readings were obtained using an ELx800 universal microplate reader (Biotek Instruments, Inc.).

Isolation and culture of primary liver cells. Mouse hepatocytes were isolated using a two-step collagenase perfusion method, as previously described (21). The cells were re-suspended in high-glucose DMEM (HyClone; Cytiva), then filtered using a 100-μm pore size cell strainer to remove undigested tissue fragments and connective tissue. The samples were then centrifuged at 50 x g for 3 min at 4˚C. The supernatant was

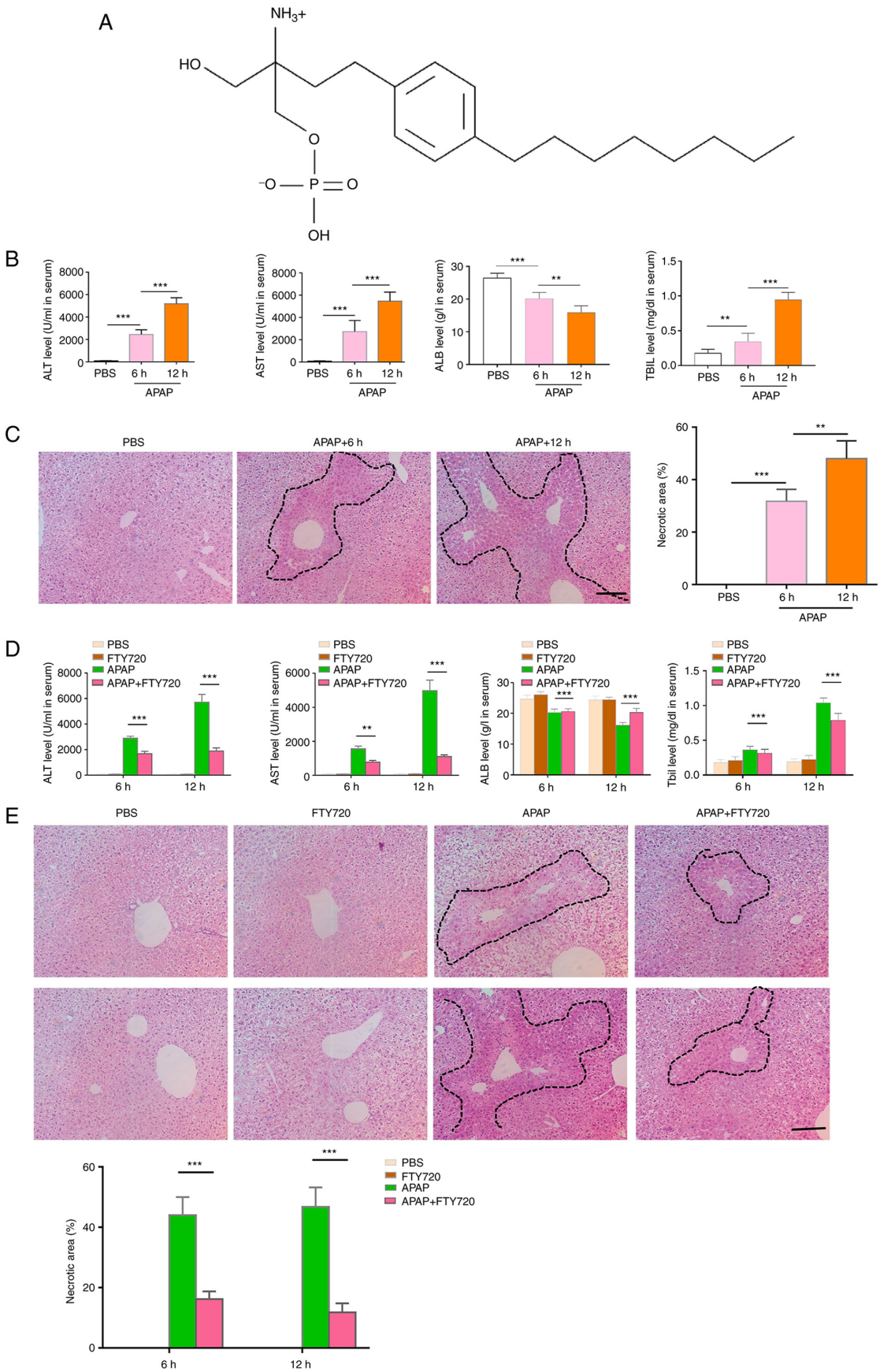

Figure 1. FTY720 alleviates APAP-induced liver injury. (A) Molecular structure of FTY720. (B) ALT, AST, ALB and TBIL levels. Mice were treated with APAP and serum was harvested 6 and 12 h post-APAP treatment. (C) H&E staining and necrotic area quantification of liver sections from APAP-treated mice. Scale bar, 200 μm. (D) Serum ALT, AST, ALB and TBIL levels in control, APAP, FTY720 and APAP + FTY720 mice. (E) H&E staining and necrotic area quantification of liver sections from control, APAP, FTY720 and APAP + FTY720 mice. Scale bar, 200 μm. The data are presented as the mean ± SEM. **P<0.01 and ***P<0.001; two-tailed, unpaired Student's t-test. APAP, acetaminophen; H&E, hematoxylin and eosin; ALT, alanine transaminase; AST, aspartate transaminase; ALB, albumin; TBIL, total bilirubin.

discarded and the cells were then re-suspended in 20 ml high-glucose DMEM. An equal volume of 90% Percoll (Cytiva) was added and mixed. The samples were then centrifuged at 200 x g for 10 min at 4˚C. The dead cells at the top of the gradient were discarded, and the cell pellet was re-suspended in 30 ml high-glucose DMEM. The centrifugation (200 x g for 3 min at 4˚C) was then repeated. The isolated hepatocytes were cultured in DMEM containing 10% FBS (Gibco; Thermo Fisher Scientific, Inc.) and 1% penicillin/streptomycin (Gibco; Thermo Fisher Scientific, Inc.) at 37˚C. Cell viability was determined using 0.4% Trypan blue staining at room temperature for 5 min.

PI staining. Primary liver cells were cultured in a 24-well culture plate for 24 h, and then stimulated with APAP (concentration, 10 mM) or FTY720 (concentration, 5 μM), or APAP + FTY720 combined for 6 h, and dead cells were stained with 1 μg/ml PI (cat. no. P4170; Sigma-Aldrich; Merck KGaA) for 5 min. The nuclei were then stained with DAPI at room temperature for 5 min. Images were obtained using Nikon eclipse TE 2000-S fluorescence microscope (Nikon Corporation). The binary processing function in ImageJ software (version 1.8.0) was used to process immunofluorescence images and measure the fluorescence parameters of cells.

Preparation of murine livers for laser scanning intravital microscopy. The mice were anesthetized with 200 mg/kg ketamine and 10 mg/kg xylazine (22). A midline and lateral incision along the costal margin to the midaxillary line was used to expose the liver. The mouse was placed in the right lateral position on the heating plate, and the ligaments connecting the liver to the diaphragm were transected to allow the liver to become exteriorized onto a glass coverslip. The blood flow was maintained. To prevent dehydration, exposed abdominal tissues were covered with a saline-soaked gauze. Neutrophils of mice at normal body temperature were stained using a rhodamine-conjugated anti-Ly-6G antibody (1:200; cat. no. PE-65140; ProteinTech Group, Inc.) for 30 min. Intravital microscopy was performed using an LSM-880 inverted microscope (Zeiss AG).

Cell viability measurement. Hepatocytes were seeded at a density of $2x10^3$ cells/well and treated with APAP (10 mM) and FTY720 (5 μM) for 6 h in a 96-well plate incubated at 37˚C with 5% CO_2. A 10-μl volume of Cell Counting Kit-8 (Dojindo Laboratories, Inc.) solution was added to the cells, which were then incubated at 37˚C with 5% CO_2 for 2 h. The optical density was measured at a wavelength of 450 nm.

Reverse transcription-quantitative PCR (RT-qPCR). Total RNA was extracted from liver tissue in TRIzol® (Takara Bio, Inc.) according to the manufacturer's protocol. First-strand cDNA synthesis was carried out using a reverse transcription kit (Takara Bio, Inc.) according to the manufacturer's protocol. SYBR® Green was used to set up the PCR using an CFX 96 Touch System (Bio-Rad Laboratories, Inc.) according to the manufacturer's instructions. The amplification conditions included 32 cycles at 95˚C for 20 sec, 57.2˚C for 30 sec, 72˚C for 30 sec and 95˚C for 2 min. qPCR was carried out using the following primers: TNF-α forward, 5'-ACGGCATGG ATCTCAAAGAC-3' and reverse, 5'-AGATAGCAAATCGGC TGACG-3'; IL-6 forward, 5'-ACAACCACGGCCTTCCCT AC-3' and reverse, 5'-TCCACGATTTCCCAGAGAACA-3'; IL-1β forward, 5'-TGTCTTGGCCGAGGACTAAGG-3' and reverse, 5'-TGGGCTGGACTGTTTCTAATGC-3'; C-C motif chemokine receptor (CCR)2 forward, 5'-TGGTAAATTCTT CAGCTTTTCC-3' and reverse, 5'-TCCACAACCTGATAA AGCCTCC-3'; CCR5 forward, 5'-CTGGCCATCTCTGAC CTGTTTTTCCTCC-3' and reverse, 5'-CAGCCCTGTGCC TCTTCTTCTCATTTC-3'; C-X-C motif chemokine ligand (CXCL)9 forward, 5'-TCCTTTTGGGCATCATCTTC-3' and reverse, 5'-TTCCCCCTCTTTTGCTTTTT-3'; C-X-C motif chemokine receptor (CXCR)2 forward, 5'-ATGCCCTCT ATTCTGCCAGAT-3' and reverse, 5'-GTGCTCCGGTTG TATAAGATGAC-3'; catalase (CAT) forward, 5'-AGGCTC AGCTGACACAGTTC-3' and reverse, 5'-ATGGAGAGACTC GGGACGAA-3'; glutathione peroxidase (GSH-PX) forward, 5'-TACAACATGTCGGACCCACG-3' and reverse, 5'-CCA GGTGGAATGAGGGCAAT-3'; total superoxide dismutase (T-SOD) forward, 5'-GCCCAAACCTATCGTGTCCA-3' and reverse, 5'-AGGGAACCCTAAATGCTGCC-3'; and GAPDH forward, 5'-TGCAGTGGCAAAGTGGAGATT-3' and reverse, 5'-TCGCTCCTGGAAGATGGTGAT-3'. qPCR assays were conducted in triplicate for each sample, and the expression levels were calculated using the $2^{-\Delta\Delta Cq}$ method (23). GAPDH was used as the housekeeping gene.

Western blot analysis. Hepatocytes were cultured in six-well plates and exposed to APAP treatment or FTY720/PBS. The cells were lysed using RIPA lysis buffer with 1 mM PMSF and 1 mM phosphatase inhibitors for 30 min on ice, then centrifuged at 500 x g for 15 min at 4˚C. The supernatant was diluted in SDS-PAGE loading buffer (the proteins were determined using BCA kits), boiled at 100˚C for 10 min, and then 20 μg of protein was loaded on 8-12% gels and transferred to a PVDF membrane (MilliporeSigma). The membranes were blocked with 5% BSA in PBS with Tween-20 (1:2,000 in PBS) for 1 h at room temperature, then incubated with primary antibodies against phosphorylated (p)-JAK2, JAK2, p-STAT3, STAT3, BAX, BCL-2 and GAPDH overnight at 4˚C. The membranes were washed 3-4 times with PBST, incubated with HRP-conjugated goat anti-mouse IgG secondary antibody (cat. no. 91196; 1:5,000; Cell Signaling Technology, Inc.) for 1-2 h at room temperature and washed again 3-4 times with PBST. The protein bands were visualized using enhanced chemiluminescence reagent (PerkinElmer, Inc.). A western blotting imaging system (Model, JP-K300; Shanghai Jiapeng Technology Co., Ltd.) was used to obtain all images. Densitometric analysis was performed using ImageJ software version 1.8.0. The list of antibodies is presented in Table I.

ROS staining. Primary hepatocytes were cultured in a 24-well culture plate for 24 h, and then stimulated with APAP (concentration, 10 mM) or FTY720 (concentration, 5 μM), or APAP + FTY720 + AG490 (concentration, 5 μM; cat. no. CSN13724; CSNpharm, Inc.) combined at 37˚C for 6 h. The primary hepatocytes were stained with 10 μmol/ml ROS-DHE (cat. no. D6883; Sigma-Aldrich; Merck KGaA) in a dark incubator at 37˚C for 30 min. ROS levels were determined by measuring the fluorescence under a fluorescence

Table I. List of antibodies.

Primary antibodies (western blotting and immunofluorescence)	Dilution	Product no.	Company
F4/80	1:500	70076	Cell Signaling Technology, Inc.
p-JAK2	1:1,000	4406	Cell Signaling Technology, Inc.
JAK2	1:1,000	3230	Cell Signaling Technology, Inc.
p-STAT3	1:1,000	52075	Cell Signaling Technology, Inc.
STAT3	1:1,000	12640	Cell Signaling Technology, Inc.
BAX	1:1,000	14796	Cell Signaling Technology, Inc.
BCL-2	1:1,000	3498	Cell Signaling Technology, Inc.
GAPDH	1:1,000	5174	Cell Signaling Technology, Inc.
p-p65	1:1,000	3033	Cell Signaling Technology, Inc.
p65	1:1,000	8242	Cell Signaling Technology, Inc.

microscope (Olympus Corporation) and analyzed using ImageJ software (version 1.8.0).

Statistical analysis. The data are presented as the mean ± SD. Data were analyzed using unpaired two-tailed Student's t-tests. Statistical analysis was carried out using SPSS software (version 23.0 for Windows; IBM Corp.). $P<0.05$ was considered to indicate a statistically significant difference.

Results

FTY720 alleviates APAP-induced liver injury. The serum levels of ALT and AST were upregulated 6 and 12 h following treatment with APAP (Fig. 1B), which indicated that excessive APAP could induce liver injury. Additionally, APAP treatment resulted in the destruction of liver tissue structure. In fact, as evidenced by H&E staining, the area of liver injury increased significantly (Fig. 1C). However, FTY720 significantly reduced the serum levels of AST and ALT at 6 and 12 h following treatment with APAP (Fig. 1D). H&E staining also indicated that FTY720 significantly reduced the area of liver injury at 6 and 12 h following treatment with APAP (Fig. 1E). These data indicated that FTY720 could alleviate the liver damage induced by APAP.

FTY720 reduces APAP-induced inflammation. Previous studies (24-26) have demonstrated that APAP-induced hepatocyte necrosis causes local inflammation and activates cells to express adhesion molecules, which promotes the recruitment of immune cells and the release of pro-inflammatory factors and chemokines, thereby aggravating liver injury.

The expression of MPO in the FTY720 + APAP group was significantly reduced compared with the APAP group (Fig. 2A). Furthermore, the effect of FTY720 on neutrophil and macrophage recruitment in APAP-induced liver injury was examined. Compared with the APAP group, macrophage recruitment was significantly reduced in the FTY720 + APAP group (Fig. 2B). *In vivo* imaging was used to directly observe the dynamic recruitment of neutrophils under different treatment conditions. A large number of neutrophils was recruited and adhered to the liver in APAP-treated mice. However, in the FTY720 + APAP group, recruitment and adhesion of neutrophils to the liver was reduced. Neutrophils were not recruited in mice treated with PBS or FTY720 alone (Videos SI-IV). In addition, FTY720 significantly reduced the expression levels of the pro-inflammatory cytokines TNF-α, IL-6 and IL-1β in damaged liver tissue (Fig. 2C). Similarly, FTY720 significantly reduced the mRNA expression of the chemokines and chemokine receptors CCR2, CCR5 and CXCL9 (Fig. 2C). These findings indicated that FTY720 reduces APAP-induced immune cell recruitment and release of pro-inflammatory cytokines and chemokines, thereby attenuating AILI.

FTY720 can activate JAK2/STAT3 signaling and inhibit apoptosis and inflammation. Previous studies have suggested that the JAK2/STAT3 signaling pathway is involved in important biological processes, such as cell proliferation, differentiation, apoptosis and immune regulation (12-14). The effect of FTY720 on the JAK2/STAT3 signaling pathway was therefore examined. APAP + FTY720 co-treatment significantly activated the JAK2/STAT3 signaling pathway compared with APAP treatment alone (Fig. 3A). Furthermore, the BAX protein expression levels were downregulated, while those of BCL-2 were upregulated in the APAP + FTY720 group compared with the APAP treatment group (Fig. 3B). In addition, FTY720 significantly reduced the activation of p65 in liver tissue compared with APAP treatment (Fig. 3C). These results indicated that FTY720 could inhibit apoptosis in hepatocytes.

FTY720 can directly protect hepatocytes against APAP-induced hepatotoxicity. To confirm whether FTY720 has a direct protective effect on hepatocytes, primary hepatocytes were treated with APAP, either alone or with FTY720. At the 6-h time-point, APAP induced hepatocyte apoptosis; however, FTY720 reversed this effect (Fig. 4A). Compared with APAP treatment, the viability of primary hepatocytes co-treated with APAP and FTY720 was increased (Fig. 4B). In addition, the JAK2/STAT3 signaling pathway was activated in primary hepatocytes co-treated with APAP and FTY720 (Fig. 4C). It was also observed that FTY720 downregulated the expression of the pro-apoptotic protein BAX and increased that of the anti-apoptotic protein BCL-2 (Fig. 4D). Thus, consistent with the *in vivo* results, FTY720 reduced hepatocyte apoptosis.

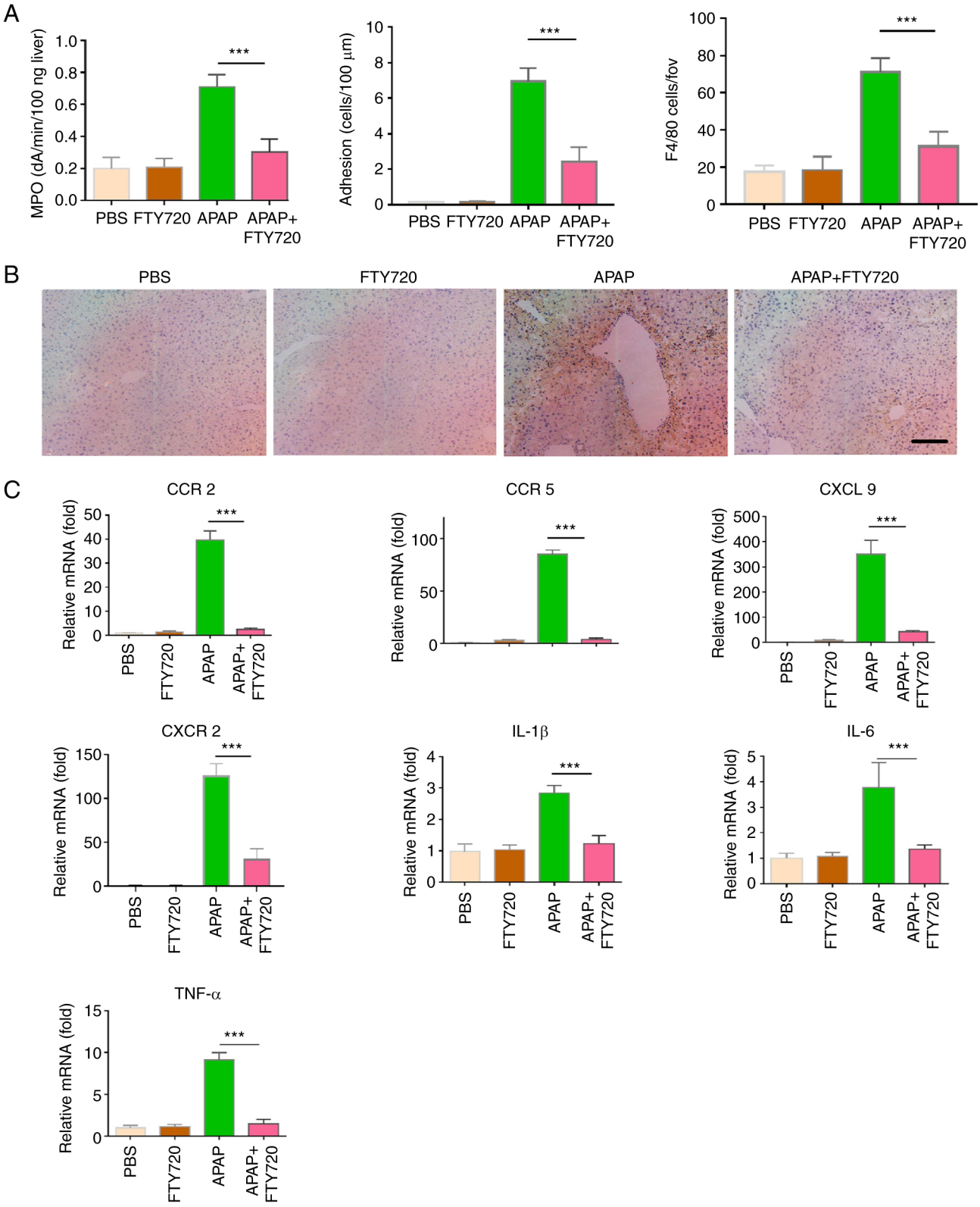

Figure 2. FTY720 reduces APAP-induced inflammation. (A) MPO levels in liver tissue lysates from control, APAP, FTY720 and APAP + FTY720 mice were measured using ELISA. (B) Infiltrating F4/80$^+$ cells in liver tissue from APAP- and FTY720 co-treated mice. Scale bar, 200 μm. (C) mRNA levels of pro-inflammatory cytokines and chemokines in liver tissue samples from control, APAP, FTY720 and APAP + FTY720 mice. The data are presented as the mean ± SEM. ***P<0.001; two-tailed, unpaired Student's t-test. APAP, acetaminophen; MPO, myeloperoxidase.

Inhibition of JAK2/STAT3 signaling attenuates the effect of FTY720 on hepatocyte apoptosis. AG490 (50 μM; 48 h), an inhibitor of the JAK2/STAT3 signaling pathway, was used in mice following the administration of APAP, either alone or together with FTY720 (Fig. 5A). In both groups, the inhibition of JAK2/STAT3 signaling resulted in a significant increase in ALT and AST (Fig. 5B). H&E staining also demonstrated that, following the inhibition of the JAK2/STAT3 signaling pathway,

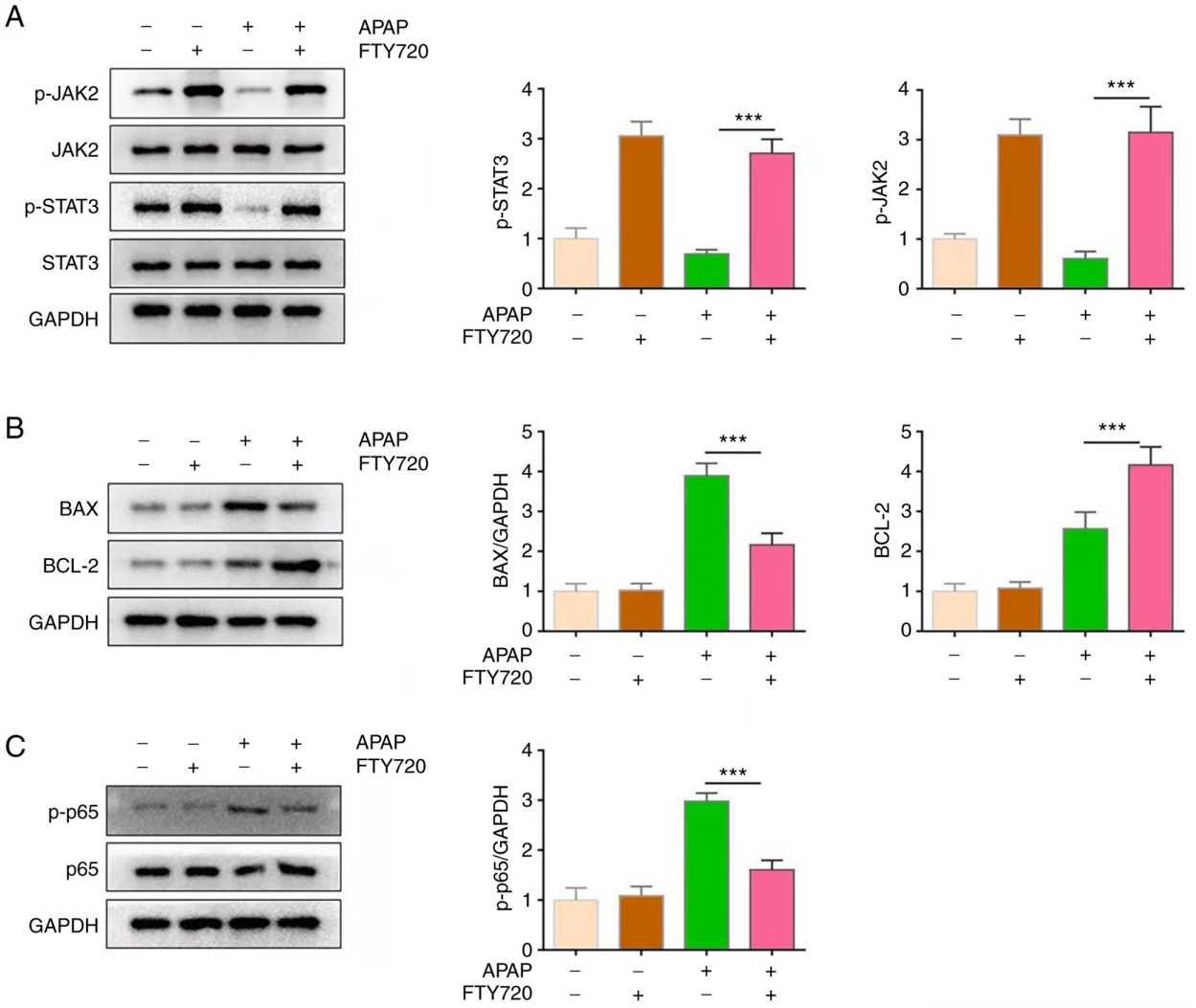

Figure 3. FTY720 inhibits apoptosis and inflammation by activating JAK2/STAT3 signaling. (A) p-JAK2, total JAK2, p-STAT3 and total STAT3 (B) BAX and BCL-2 and (C) p-p65 and total p65 protein levels in liver tissue from control, APAP, FTY720 and APAP + FTY720 mice. The data are presented as the mean ± SEM. ***P<0.001; two-tailed, unpaired Student's t-test. APAP, acetaminophen; JAK2, Janus kinase 2; p-, phosphorylated.

the area of damaged liver tissue significantly increased in both groups (Fig. 5C). In addition, neutrophil recruitment and the survival rate were also significantly increased (Fig. 5D and E, respectively). These data suggested that the JAK2/STAT3 signaling pathway may mediate the effects of FTY720 on hepatocytes.

Inhibition of JAK2/STAT3 signaling attenuates the effect of FTY720 on oxidative stress. Oxidative stress resulting from APAP-induced hepatocyte apoptosis can aggravate liver injury. The oxidative stress level of primary hepatocytes decreased significantly following co-treatment with APAP and FTY720, although this effect was reversed by AG490 (Fig. 6A). Moreover, the mRNA expression levels of CAT, GSH-PX and T-SOD, which are markers of oxidative stress, increased significantly following FTY720 treatment and were significantly downregulated by AG490 (Fig. 6B). These data suggested that FTY720 inhibits APAP-induced oxidative stress by regulating the JAK2/STAT3 signaling pathway. In summary, APAP led to hepatocyte apoptosis and increased neutrophil and macrophage recruitment, further aggravating liver injury. FTY720 can reverse APAP-induced liver cell apoptosis, excessive oxidative stress injury and neutrophil and macrophage recruitment by the activating JAK2/STAT3 signaling pathway, thereby attenuating liver injury (Fig. 6C).

Discussion

The improper use of health products, such as prescription medicines, over-the-counter drugs and traditional Chinese medicines, can cause varying degrees of liver damage (27). The incidence of drug-induced liver injury (DILI) has been increasing in recent years (28). In the process of DILI, drugs and their metabolites combine with endogenous hepatocyte components to form new complexes, which activate hepatocytes and lead to hepatocyte injury or even death (29,30). In China, DILI accounts for ~10% of hospitalized patients with acute hepatitis. Clinical screening also suggests that 20-50% of the adults with elevated transaminase levels suffer from DILI (31). Therefore, DILI has become a common clinical liver disease.

It has been reported that excessive APAP intake leads to the accumulation of the toxic metabolite NAPQI in hepatocytes (32).

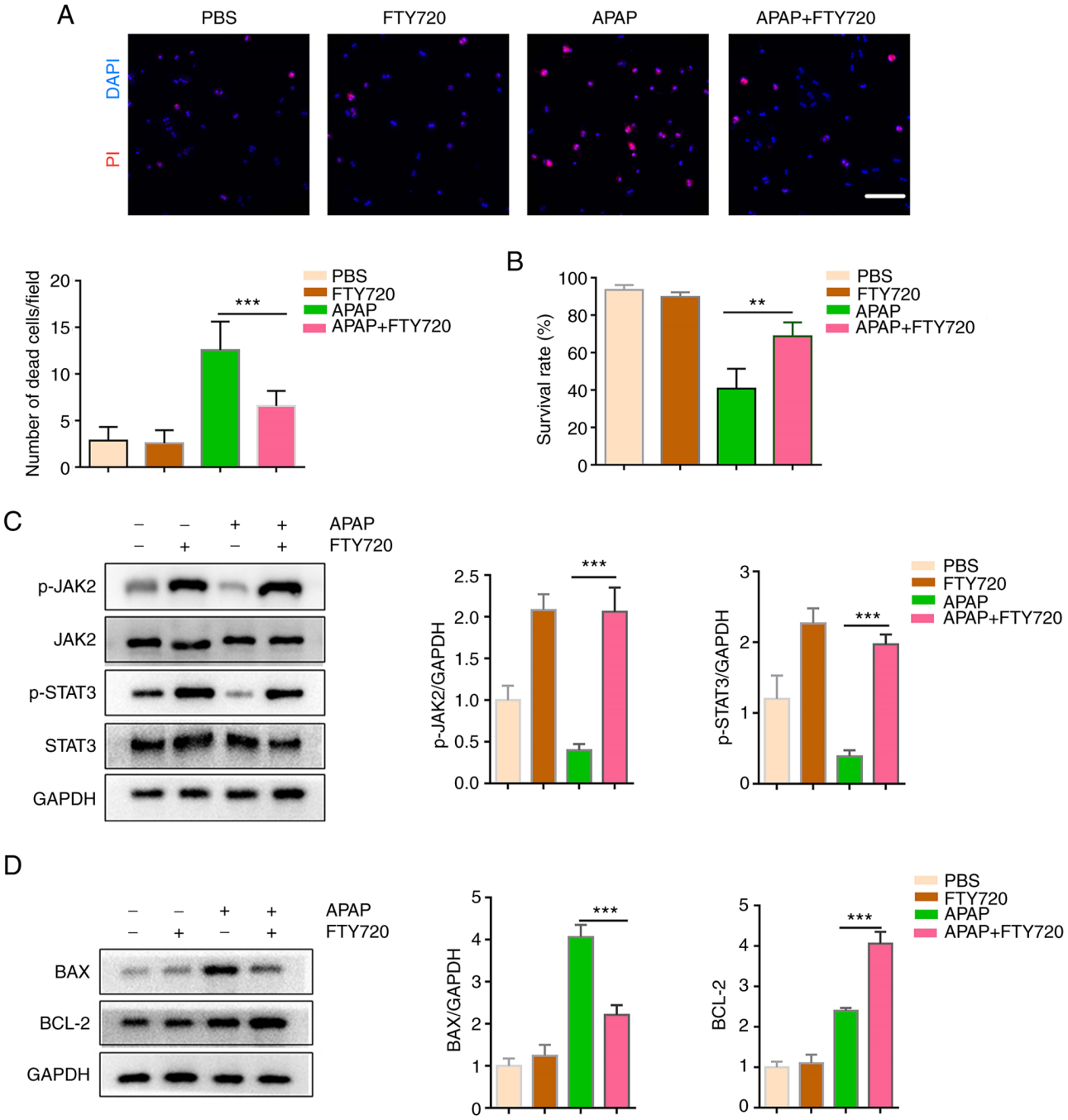

Figure 4. FTY720 alleviates APAP-induced hepatotoxicity. Primary hepatocytes from mice were treated with 10 mM APAP and 5 μM FTY720. (A) Cell death was analyzed using propidium iodide staining. (B) Cell viability was analyzed using Cell Counting Kit-8 assays. (C) p-JAK2, total JAK2, p-STAT3 and total STAT3 protein abundance in APAP- and FTY720-treated hepatocytes. (D) BAX and BCL-2 protein expression levels in APAP- and FTY720-treated hepatocytes. The data are presented as the mean ± SEM. **P<0.01 and ***P<0.001; two-tailed, unpaired Student's t-test. APAP, acetaminophen; JAK2, Janus kinase 2; p-, phosphorylated.

The accumulation of NAPQI downregulates glutathione in hepatocytes; NAQPI also binds to outer mitochondrial membrane proteins (4,33). The covalent binding of NAPQI to mitochondrial proteins leads to oxidative stress and the opening of mitochondrial membrane permeability transition pore, which leads to reduced mitochondrial membrane potential, mitochondrial function and ATP production in hepatocytes. This results in lipid peroxidation, oxidative stress and DNA fragmentation, leading to the necrosis of hepatocytes (24). Following hepatocyte necrosis, a large number of damage-associated molecular patterns and chemokines are released, thereby activating Kupffer cells located in the liver and recruiting macrophages and neutrophils from the peripheral circulation to the site of liver injury (25,26). This results in aseptic inflammation, further aggravating liver injury (7,34). Taken together all aforementioned studies have revealed that APAP-induced liver injury is a very complex pathophysiological process, involving inflammation, apoptosis and neutrophil infiltration.

In the present study, neutrophil infiltration into the liver was observed following intraperitoneal injection of APAP in

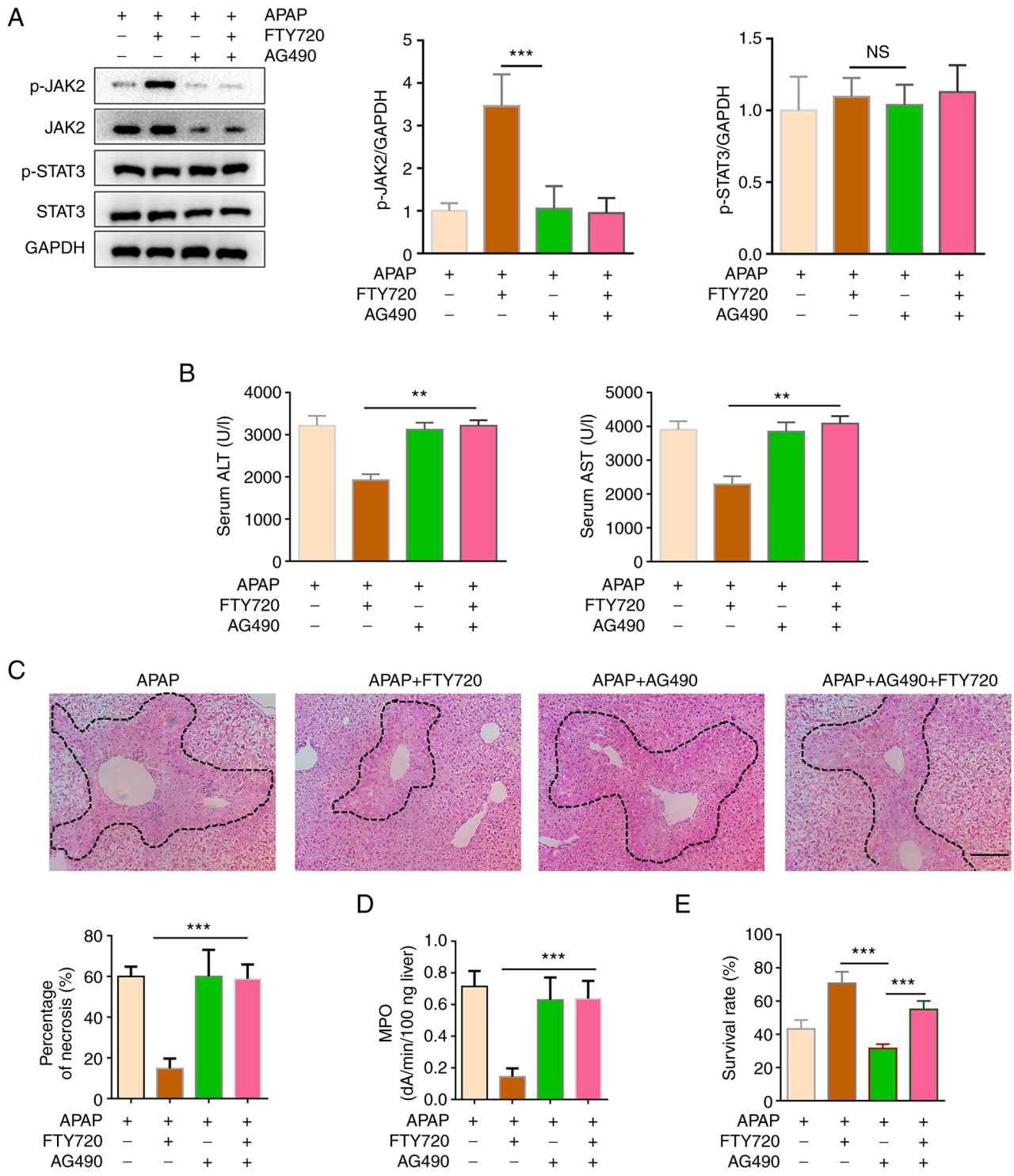

Figure 5. Inhibition of JAK2/STAT3 weakens the protective effect of FTY720. Mice were treated with APAP, with or without FTY720 and AG490. (A) p-JAK2, total JAK2, p-STAT3 and total STAT3 protein abundance were analyzed by western blotting. (B) Serum ALT and AST levels were assayed by commercial kits. (C) Hematoxylin and eosin staining and necrotic area quantification of liver sections. Scale bar, 200 μm. (D) MPO levels were determined in liver tissue lysates using ELISA. (E) Cell viability was analyzed using Cell Counting Kit-8 assays. The data are presented as the mean ± SEM. **P<0.01 and ***P<0.001; two-tailed, unpaired Student's t-test. APAP, acetaminophen; JAK2, Janus kinase 2; ALT, alanine transaminase; AST, aspartate transaminase; MPO, myeloperoxidase; NS, not significant.

mice. However, when FTY720 and APAP were co-administered, the number of neutrophils infiltrating the liver was significantly reduced compared with that of the APAP group. Another study has suggested that FTY720 induces neutrophil extracellular traps through an NADPH oxidase-independent pathway and that this compound could represent a potential antibacterial drug (35). FTY720 is an S1P analog and a potent S1P receptor modulator. It induces the internalization of S1P1 and consequently inhibits S1P activity. Previous studies have also confirmed that S1P prevents egress of hematopoietic

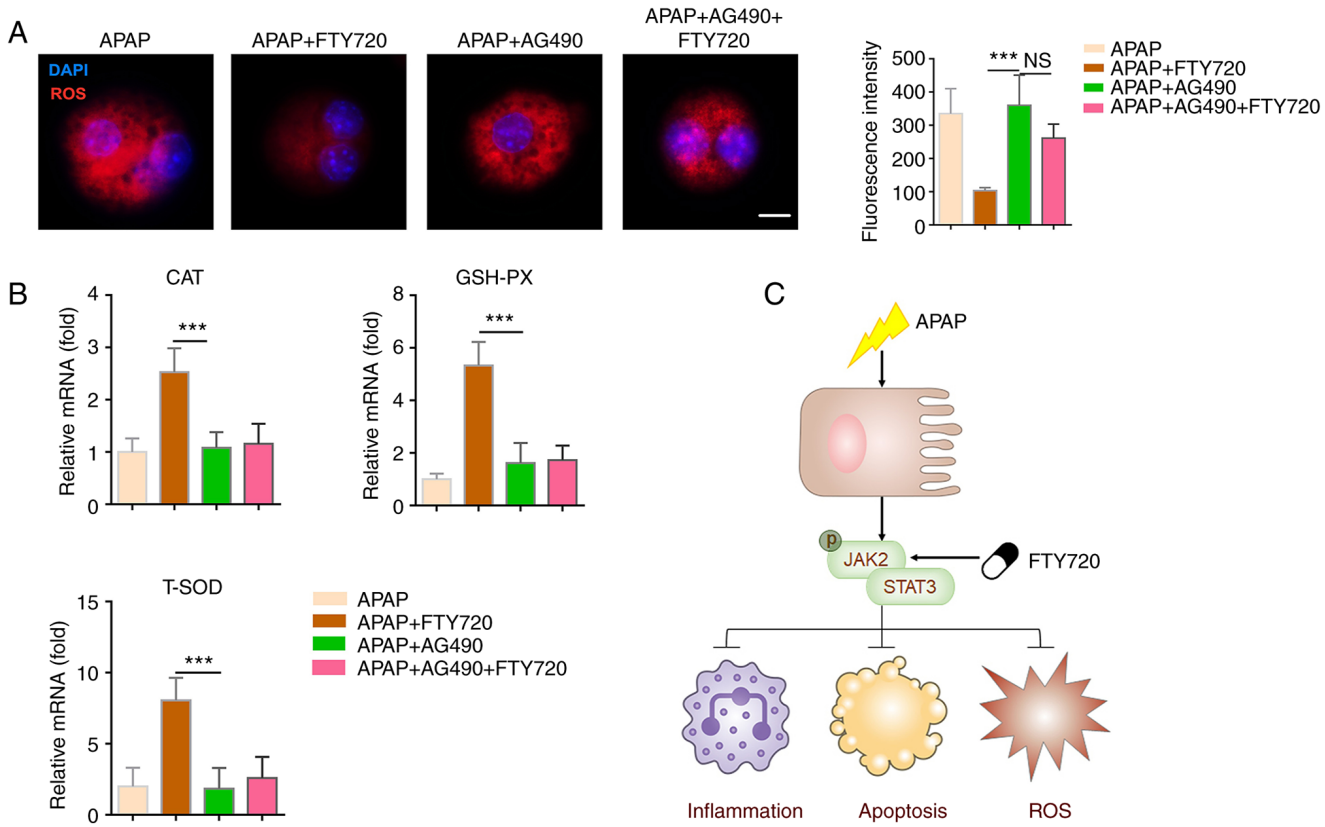

Figure 6. Inhibition of JAK2/STAT3 signaling attenuates the effects of FTY720. (A) Primary murine hepatocytes were treated with APAP, with or without FTY720 and AG490. The levels of ROS were analyzed using a commercial kit. Scale bar, 20 μm. (B) mRNA levels of CAT, GSH-PX and T-SOD in liver tissue. (C) Schematic illustration of the putative signaling mechanism. The data are presented as the mean ± SEM. ***P<0.001; two-tailed, unpaired Student's t-test. APAP, acetaminophen; JAK2, Janus kinase 2; GSH-PX, glutathione peroxidase; T-SOD, total superoxide dismutase; ROS, reactive oxygen species; CAT, catalase; NS, not significant.

stem cells from the liver to reduce fibrosis and suppresses TLR-induced CXCL8 secretion from human T cells (36,37). Liang *et al* (38) reported that CXCL9/10 possesses antifibrotic roles on liver non-parenchymal cells. In previous studies the depletion of peripheral T cells by FTY720 resulted in increased infiltration of innate immune cells concomitant to reduced T-cell infiltration and exacerbation of hypoxic-ischemic-induced brain injury, which indicates that neonatal T cells may promote endogenous neuroprotection in the term-born equivalent hypoxic-ischemic brain potentially providing new opportunities for therapeutic intervention (39,40). It may be hypothesized that FTY720 could directly affect the recruitment of neutrophils and macrophages that express S1P receptors. FTY720 is a novel type of immunosuppressant derived from the ascomycete *Cordyceps sinensis*, which plays an important role in immunosuppression by inducing lymphocyte apoptosis and homing (41,42). Furthermore, it has been reported that rat spleen cells cultured with FTY720 displayed the typical characteristics of apoptosis, including disappearance of microvilli on the cell surface, concentration of chromatin and the formation of apoptotic bodies (43). Human lymphocytes co-treated with FTY720 exhibit the same features. Nagahara *et al* (44) suggested that FTY720 induced lymphocyte apoptosis through changes in membrane permeability and the release of cytochrome *c* from cells. However, other studies have shown that the molecular mechanism of lymphocyte apoptosis was complex and resulted from a variety of factors (45,46). Due to the downregulation of the BCL-2 protein and upregulation of the BAX protein, it may be suggested that the BCL-2 family is involved in FTY720-induced lymphocyte apoptosis. In the present study, FTY720 reversed the BAX/BCL-2 ratio and APAP-induced oxidative stress. It has been demonstrated that FTY720 could inhibit the proliferation of glomerular mesangial cells by inducing cell cycle arrest and apoptosis, possibly via the regulation of the expression of cell cycle-related genes and BAX/BCL-2 (47). In addition, exosomes could ameliorate the morphology of neurons, reduce inflammatory infiltration and edema, decrease the expression of BAX and AQP-4, upregulate the expression of claudin-5 and BCL-2 and inhibit cell apoptosis (48).

In the present study, AILI led to hepatocyte apoptosis and upregulation of pro-inflammatory factors, indicative of activation of the innate immune system. IL family members (IL-6, -13 and -22) can effectively activate STAT3 during the process of liver repair. STAT3 is an essential signaling molecule that can directly or indirectly regulate the expression of important genes in the process of liver repair (49). STAT3 is mainly coupled with JAK tyrosine protein kinases and participates in the signal transduction process downstream of extracellular signals, such as ILs; with significant anti-apoptotic and pro-mitotic effects (50). It has also been found that pro-inflammatory factors can activate and phosphorylate JAK2, further induce STAT3 phosphorylation, thus participating in the regulation of gene transcription and mediating the expression of a

variety of pro-inflammatory factors (51). Therefore, detecting the serum levels of IL-6, -13 and -22, as well as the expression of STAT3 and JAK2 in liver tissue can provide insight into the effect of FTY720 on AILI.

However, there is a limitation in the present study. FTY720 hydrochloride is an analog of sphingosine and a potent modulator of S1P receptors. FTY720 hydrochloride is phosphorylated by sphingosine kinases, particularly by SK2, and then binds S1PR1, 3, 4, and 5. FTY720 hydrochloride induces the internalization of S1P1, and consequently, inhibits S1P activity (52-54). S1P was not analyzed in the present study. Therefore, S1P could be analyzed in the future.

In conclusion, FTY720 could significantly ameliorate AILI. FTY720 was able to inhibit the metabolism of APAP oxidase and reduce the production of NAPQI; it could also inhibit the oxidative stress produced by mitochondrial permeability transition to reduce hepatocyte death. FTY720 also reduced the infiltration of neutrophils into the liver, thereby reducing AILI in mice. FTY720 may serve this protective role by regulating the JAK2/STAT3 signaling pathway. The present findings revealed a novel mechanism through which FTY720 attenuates AILI and provide a theoretical basis for the clinical treatment of AILI using this compound.

Acknowledgements

Not applicable.

Funding

No funding was received.

Availability of data and materials

The datasets used and/or analyzed during the current study are available from the corresponding author on reasonable request.

Authors' contributions

XH and BC designed the study and carried out the experiments. KK, DP and YS analyzed the data, as well as wrote and edited the manuscript. All authors have read and approved the final manuscript and confirm the authenticity of all the raw data.

Ethics approval and consent to participate

Experiments were conducted under protocols approved (approval no. CMU2021076) by the Institutional Animal Care and Use Committee and conformed to the Guidelines for the Care and Use of Laboratory Animals of China Medical University (Shenyang, China).

Patient consent for publication

Not applicable.

Competing interests

The authors declare that they have no competing interests.

References

1. Shan S, Shen Z and Song F: Autophagy and acetaminophen-induced hepatotoxicity. Arch Toxicol 92: 2153-2161, 2018.
2. Bernal W and Wendon J: Acute liver failure. N Engl J Med 369: 2525-2534, 2013.
3. Bunchorntavakul C and Reddy KR: Acetaminophen (APAP or N-Acetyl-p-Aminophenol) and acute liver failure. Clin Liver Dis 22: 325-346, 2018.
4. Fisher ES and Curry SC: Evaluation and treatment of acetaminophen toxicity. Adv Pharmacol 85: 263-272, 2019.
5. Jóźwiak-Bebenista M and Nowak JZ: Paracetamol: Mechanism of action, applications and safety concern. Acta Pol Pharm 71: 11-23, 2014.
6. Ramachandran A and Jaeschke H: Acetaminophen toxicity: Novel insights into mechanisms and future perspectives. Gene Expr 18: 19-30, 2018.
7. Ramachandran A and Jaeschke H: Acetaminophen hepatotoxicity. Semin Liver Dis 39: 221-234, 2019.
8. He Y, Feng D, Li M, Gao Y, Ramirez T, Cao H, Kim SJ, Yang Y, Cai Y, Ju C, *et al*: Hepatic mitochondrial DNA/Toll-like receptor 9/MicroRNA-223 forms a negative feedback loop to limit neutrophil overactivation and acetaminophen hepatotoxicity in mice. Hepatology 66: 220-234, 2017.
9. Guo XD, Ji J, Xue TF, Sun YQ, Guo RB, Cheng H and Sun XL: FTY720 exerts anti-glioma effects by regulating the glioma microenvironment through increased CXCR4 internalization by glioma-associated microglia. Front Immunol 11: 178, 2020.
10. Dragun D, Fritsche L, Boehler T, Peters H, Budde K and Neumayer HH: FTY720: Early clinical experience. Transplant Proc 36 (2 Suppl): 544S-548S, 2004.
11. Marciniak A, Camp SM, Garcia JGN and Polt R: An update on sphingosine-1-phosphate receptor 1 modulators. Bioorg Med Chem Lett 28: 3585-3591, 2018.
12. Cheng X, Yeung PKK, Zhong K, Zilundu PLM, Zhou L and Chung SK: Astrocytic endothelin-1 overexpression promotes neural progenitor cells proliferation and differentiation into astrocytes via the Jak2/Stat3 pathway after stroke. J Neuroinflammation 16: 227, 2019.
13. Jo S, Wang SE, Lee YL, Kang S, Lee B, Han J, Sung IH, Park YS, Bae SC and Kim TH: IL-17A induces osteoblast differentiation by activating JAK2/STAT3 in ankylosing spondylitis. Arthritis Res Ther 20: 115, 2018.
14. Zhang L and Wei W: Anti-inflammatory and immunoregulatory effects of paeoniflorin and total glucosides of paeony. Pharmacol Ther 207: 107452, 2020.
15. Hata T, Rehman F, Hori T and Nguyen JH: GABA, γ-aminobutyric acid, protects against severe liver injury. J Surg Res 236: 172-183, 2019.
16. Yu HC, Qin HY, He F, Wang L, Fu W, Liu D, Guo FC, Liang L, Dou KF and Han H: Canonical notch pathway protects hepatocytes from ischemia/reperfusion injury in mice by repressing reactive oxygen species production through JAK2/STAT3 signaling. Hepatology 54: 979-988, 2011.
17. Zai W, Chen W, Luan J, Fan J, Zhang X, Wu Z, Ding T, Ju D and Liu H: Dihydroquercetin ameliorated acetaminophen-induced hepatic cytotoxicity via activating JAK2/STAT3 pathway and autophagy. Appl Microbiol Biotechnol 102: 1443-1453, 2018.
18. Freitas MC, Uchida Y, Zhao D, Ke B, Busuttil RW and Kupiec-Weglinski JW: Blockade of Janus kinase-2 signaling ameliorates mouse liver damage due to ischemia and reperfusion. Liver Transpl 16: 600-610, 2010.
19. Zhou HC, Wang H, Shi K, Li JM, Zong Y and Du R: Hepatoprotective effect of baicalein against acetaminophen-induced acute liver injury in mice. Molecules 24: 131, 2018.
20. Hong SS, Choi JH, Lee SY, Park YH, Park KY, Lee JY, Kim J, Gajulapati V, Goo JI, Singh S, *et al*: A novel small-molecule inhibitor targeting the IL-6 receptor β subunit, glycoprotein 130. J Immunol 195: 237-245, 2015.
21. Wright MC, Issa R, Smart DE, Trim N, Murray GI, Primrose JN, Arthur MJ, Iredale JP and Mann DA: Gliotoxin stimulates the apoptosis of human and rat hepatic stellate cells and enhances the resolution of liver fibrosis in rats. Gastroenterology 121: 685-698, 2001.
22. Liew PX, Lee WY and Kubes P: iNKT cells orchestrate a switch from inflammation to resolution of sterile liver injury. Immunity 47: 752-765.e5, 2017.
23. Livak KJ and Schmittgen TD: Analysis of relative gene expression data using real-time quantitative PCR and the 2(-Delta Delta C(T)) method. Methods 25: 402-408, 2001.

24. Athersuch TJ, Antoine DJ, Boobis AR, Coen M, Daly AK, Possamai L, Nicholson JK and Wilson ID: Paracetamol metabolism, hepatotoxicity, biomarkers and therapeutic interventions: A perspective. Toxicol Res (Camb) 7: 347-357, 2018.
25. Mitchell JR, Jollow DJ, Potter WZ, Gillette JR and Brodie BB: Acetaminophen-induced hepatic necrosis. IV. Protective role of glutathione. J Pharmacol Exp Ther 187: 211-217, 1973.
26. Giustarini G, Kruijssen L, van Roest M, Bleumink R, Weaver RJ, Bol-Schoenmakers M, Smit J and Pieters R: Tissue influx of neutrophils and monocytes is delayed during development of trovafloxacin-induced tumor necrosis factor-dependent liver injury in mice. J Appl Toxicol 38: 753-765, 2018.
27. Lesiński W, Mnich K, Golińska AK and Rudnicki WR: Integration of human cell lines gene expression and chemical properties of drugs for drug induced liver injury prediction. Biol Direct 16: 2, 2021.
28. Kong X, Guo D, Liu S, Zhu Y and Yu C: Incidence, characteristics and risk factors for drug-induced liver injury in hospitalized patients: A matched case-control study. Br J Clin Pharmacol 87: 4304-4312, 2021.
29. Katarey D and Verma S: Drug-induced liver injury. Clin Med (Lond) 16 (Suppl 6): S104-S109, 2016.
30. Fisher K, Vuppalanchi R and Saxena R: Drug-induced liver injury. Arch Pathol Lab Med 139: 876-887, 2015.
31. Shen T, Liu Y, Shang J, Xie Q, Li J, Yan M, Xu J, Niu J, Liu J, Watkins PB, *et al*: Incidence and etiology of drug-induced liver injury in mainland China. Gastroenterology 156: 2230-2241.e11, 2019.
32. Jaeschke H, Murray FJ, Monnot AD, Jacobson-Kram D, Cohen SM, Hardisty JF, Atillasoy E, Hermanowski-Vosatka A, Kuffner E, Wikoff D, *et al*: Assessment of the biochemical pathways for acetaminophen toxicity: Implications for its carcinogenic hazard potential. Regul Toxicol Pharmacol 120: 104859, 2021.
33. Papp S, Moderzynski K, Rauch J, Heine L, Kuehl S, Richardt U, Mueller H, Fleischer B and Osterloh A: Liver necrosis and lethal systemic inflammation in a murine model of rickettsia typhi Infection: Role of neutrophils, macrophages and NK cells. PLoS Negl Trop Dis 10: e0004935, 2016.
34. Ishitsuka Y, Kondo Y and Kadowaki D: Toxicological property of acetaminophen: The dark side of a safe antipyretic/analgesic drug. Biol Pharm Bull 43: 195-206, 2020.
35. Zhang L, Gao H, Yang L, Liu T, Zhang Q, Xun J, Li C, Cui L and Wang X: FTY720 induces neutrophil extracellular traps via a NADPH oxidase-independent pathway. Arch Biochem Biophys 711: 109015, 2021.
36. King A, Houlihan DD, Kavanagh D, Haldar D, Luu N, Owen A, Suresh S, Than NN, Reynolds G, Penny J, *et al*: Sphingosine-1-phosphate prevents egress of hematopoietic stem cells from liver to reduce fibrosis. Gastroenterology 153: 233-248.e16, 2017.
37. Sharma N, Akhade AS and Qadri A: Sphingosine-1-phosphate suppresses TLR-induced CXCL8 secretion from human T cells. J Leukoc Biol 93: 521-528, 2013.
38. Liang YJ, Luo J, Lu Q, Zhou Y, Wu HW, Zheng D, Ren YY, Sun KY, Wang Y and Zhang ZS: Gene profile of chemokines on hepatic stellate cells of schistosome-infected mice and antifibrotic roles of CXCL9/10 on liver non-parenchymal cells. PLoS One 7: e42490, 2012.
39. Herz J, Köster C, Crasmöller M, Abberger H, Hansen W, Felderhoff-Müser U and Bendix I: Peripheral T cell depletion by FTY720 exacerbates hypoxic-ischemic brain injury in neonatal mice. Front Immunol 9: 1696, 2018.
40. Sola A, Weigert A, Jung M, Vinuesa E, Brecht K, Weis N, Brüne B, Borregaard N and Hotter G: Sphingosine-1-phosphate signalling induces the production of Lcn-2 by macrophages to promote kidney regeneration. J Pathol 225: 597-608, 2011.
41. Tsai HC and Han MH: Sphingosine-1-Phosphate (S1P) and S1P signaling pathway: Therapeutic targets in autoimmunity and inflammation. Drugs 76: 1067-1079, 2016.
42. Zhao M, Yang C, Chai S, Yuan Y, Zhang J, Cao P, Wang Y, Xiao X, Wu K, Yan H, *et al*: Curcumol and FTY720 synergistically induce apoptosis and differentiation in chronic myelomonocytic leukemia via multiple signaling pathways. Phytother Res 35: 2157-2170, 2021.
43. Takai K, Takahara S, Isoyama N, Tsuchida M, Matsumura M, Kishi Y, Uchiyama K and Naito K: Effects of FTY720 on rat lymphoid organs. Transplant Proc 36: 2453-2456, 2004.
44. Nagahara Y, Enosawa S, Ikekita M, Suzuki S and Shinomiya T: Evidence that FTY720 induces T cell apoptosis in vivo. Immunopharmacology 48: 75-85, 2000.
45. Tuckermann JP, Kleiman A, McPherson KG and Reichardt HM: Molecular mechanisms of glucocorticoids in the control of inflammation and lymphocyte apoptosis. Crit Rev Clin Lab Sci 42: 71-104, 2005.
46. Sordo-Bahamonde C, Lorenzo-Herrero S, Payer ÁR, Gonzalez S and López-Soto A: Mechanisms of apoptosis resistance to NK cell-mediated cytotoxicity in cancer. Int J Mol Sci 21: 3726, 2020.
47. Jiang J, Huang X, Wang Y, Deng A and Zhou J: FTY720 induces cell cycle arrest and apoptosis of rat glomerular mesangial cells. Mol Biol Rep 39: 8243-8250, 2012.
48. Chen J, Zhang C, Li S, Li Z, Lai X and Xia Q: Exosomes derived from nerve stem cells loaded with FTY720 promote the recovery after spinal cord injury in rats by PTEN/AKT signal pathway. J Immunol Res 2021: 8100298, 2021.
49. Hu Z, Han Y, Liu Y, Zhao Z, Ma F, Cui A, Zhang F, Liu Z, Xue Y, Bai J, *et al*: CREBZF as a key regulator of STAT3 pathway in the control of liver regeneration in mice. Hepatology 71: 1421-1436, 2020.
50. Ozaki M: Cellular and molecular mechanisms of liver regeneration: Proliferation, growth, death and protection of hepatocytes. Semin Cell Dev Biol 100: 62-73, 2020.
51. Zegeye MM, Lindkvist M, Fälker K, Kumawat AK, Paramel G, Grenegård M, Sirsjö A and Ljungberg LU: Activation of the JAK/STAT3 and PI3K/AKT pathways are crucial for IL-6 trans-signaling-mediated pro-inflammatory response in human vascular endothelial cells. Cell Commun Signal 16: 55, 2018.
52. Foster AD, Vicente D, Clark N, Leonhardt C, Elster EA, Davis TA and Bradley MJ: FTY720 effects on inflammation and liver damage in a rat model of renal ischemia-reperfusion injury. Mediators Inflamm 2019: 3496836, 2019.
53. Zhao Y, Man K, Lo CM, Ng KT, Li XL, Sun CK, Lee TK, Dai XW and Fan ST: Attenuation of small-for-size liver graft injury by FTY720: Significance of cell-survival Akt signaling pathway. Am J Transplant 4: 1399-1407, 2004.
54. Kaneko T, Murakami T, Kawana H, Takahashi M, Yasue T and Kobayashi E: Sphingosine-1-phosphate receptor agonists suppress concanavalin A-induced hepatic injury in mice. Biochem Biophys Res Commun 345: 85-92, 2006.